14th Australasian Fluid Mechanics Conference
Adelaide University, Adelaide, Australia
10-14 December 2001

Measurements of Gap Velocity in a Heart Pump Model

L.P.Chua, K.S.Ong, S.C.M.Yu, W.K.Chan and Y.W.Wong

School of Mechanical and Production Engineering

Nanyang Technological University, 50 Nanyang Avenue, Singapore 639798

Abstract

Animal trials of the Kyoto-NTN Magnetically Suspended Centrifugal Blood Pump (MSCP) showed that hemolysis and thrombosis were prevalent in the clearance gaps between the impeller shroud surfaces and pump casing. This paper presents the measurement of the velocity in the clearance gap of a 5:1 model of the pump. The velocity vector distributions show that the double volute design of the pump, especially the splitter plate that started at $\theta = 180^o$ has created a washout mechanism in the clearance gap. These have suggested that hemolysis and thrombus formations are minimal and hence the pump is able to function nominally efficient as compared to other centrifugal pumps.

Introduction

Centrifugal pump is widely used as ventricle assist device because of its simpler design and ease of handling. The centrifugal blood pump for present study is an extension of the research group at Kyoto University, Japan. Figure 1 shows the schematic of the centrifugal blood pump that have been investigated in this study which was developed by Kyoto University since 1989 [1,2].

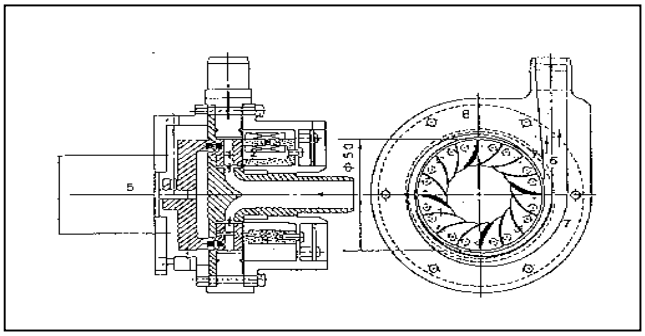

Figure 1. Schematic of the Kyoto University magnetically suspended artificial heart pump

The MSCP has shown its superiority over other heart pumps. However, significant hemolysis and thrombosis have been revealed prevalent in the 0.2 mm clearance gap between the impeller and the pump casing in vivo testing [3]. The objective of this study is thus to present the gap velocity measurements in the clearance gap. With the velocity distributions, a better and more detail observation of the flow field in the gap can be achieved and therefore the mechanism of thrombus formation and hemolysis can be understood. However, it is difficult and nearly impossible to measure the velocity inside the 0.2 mm gap. In order to have the measurements in the gap made efficiently, modifications on the pump are needed. By applying dimensional analysis and pump similarity law, the prototype was scaled up 5 times, increasing the gap from 0.2mm to 1mm [4]. Air was used as the fluid medium in this preliminary study and the tangential (v) and radial (u) velocity measurements were done by the hot wire anemometer.

Method

To facilitate the gap velocity measurement, the pump front volute has been modified and is shown in Figure 2. Briefly, the front volute cover is a separate piece from the front volute and it is allowed to be rotated freely. There were seven holes drilled across the diameter of the front volute cover of the pump at radius (in mm) r = 69.5, 78, 86.5, 95, 103.5, 112 and 120.5 for measurements.

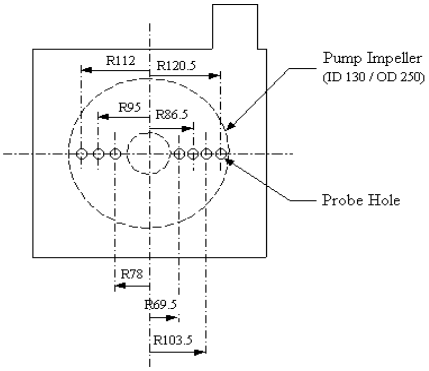

Figure 2. Schematic diagram of the model pump with 7 radial positions

The probes for the velocity measurement consists of a hot wire and a cold wire, soldered on 2 sharp prongs at different z (the distances of the sensing elements from the base of the probe (in mm)) of 0.25, 0.50 and 0.75. The hot wire (ϕ5μm Wollaston Pt 10%-Rh), for velocity measurement, is operated under CTA to measure velocity, and the cold-wire (ϕ5μm Wollaston Pt 10%-Rh), is operated under CCA to measure temperature [5]. Both wires have the active length l of 1 mm. The cold wire is required here to account for the temperature differences between calibration and measurement environment of hot wire as the air in the model will be heated after running in the pump for sometime.

A rotating disk apparatus as shown in Figure 3 was used for the calibration of the hot wire and the determination of the temperature compensation [6]. It consists of a stationary disk, a rotating disk and a motor. A detailed description of the calibration rig can be found in [7]. For calibration, the probe is mounted flush at a fixed radial position on the stationary plate while the rotating disk is facing but kept at a constant distance away from the probe.

The tangential (v) and radial (u) velocity (m/s) can be expressed as [8]

$$v = \omega r\left[\xi - \mathrm{Re}^2\left(8\xi + 35\xi^4 - 63\xi^5 + 20\xi^7\right)/\,6300\right] \quad (1)$$

$$u = -\omega r\,\mathrm{Re}\left(4\xi - 9\xi^2 + 5\xi^4\right)/\,60 \quad (2)$$

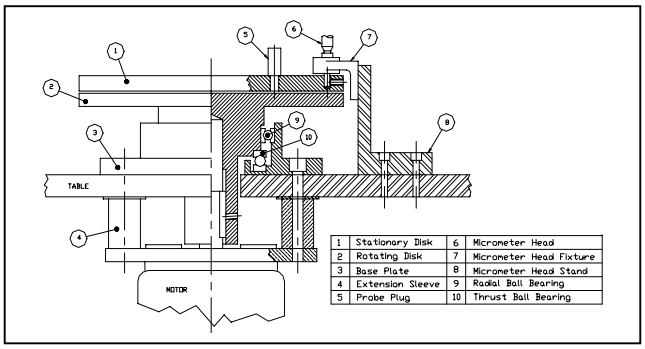

Figure 3. Probe calibration rig arrangement

where Re is the Reynolds number ($=\omega d^2/\nu$), ν is the kinematics viscosity, d is the gap width between plates, ω is the angular velocity of rotating plate, r is the radial location of the probe, ξ (=z/d) is the non-dimensional distance from fixed disk.

By varying the three parameters (*r*, ω and *d*) in Eq. (1) or (2), the calibration constants *A, B* and n between fluid velocity and probe output voltage *E* can be determined by [9]

$$E^2 = A + BU^n \tag{3}$$

where E is the CTA voltage (V), U is the velocity of the flow and it could be either the tangential velocity v or the radial velocity u depending on the orientation of the probe (see Figure 4).

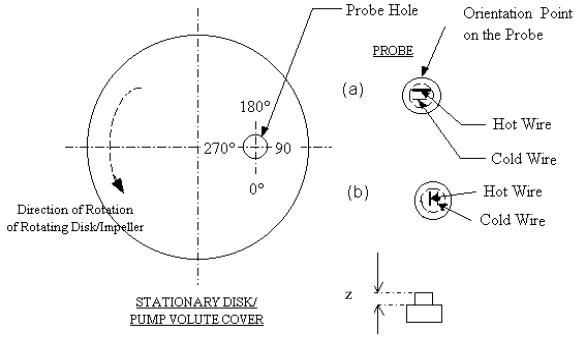

Figure 4. Probe orientation with the direction of rotatin of the flow for (a) tangential velocity v and (b) radial velocity u.

The difference in temperature between calibration and measurement due to air viscosity is accounted for through [5]

$$E_c = E + \left.\frac{\partial E}{\partial T}\right|_U (\Delta T) \tag{4}$$

where E_c is the temperature compensated CTA voltage (V), $\left.\frac{\partial E}{\partial T}\right|_U$ is the change of CTA voltage due to the change of temperature at constant U (V/K) and ΔT is the difference in temperature (K).

The temperature difference Δ*T,* between the reference (ambient) and measurement point, is given by

$$\Delta T = \frac{GIR\alpha}{\Delta V} \tag{5}$$

where ΔT is the temperature change with respect to the reference temperature (K), *G* is the set gain on the CCA (x1000), I is the set current on the CCA (mA), *R* is the wire cold resistance (Ω), α is the wire temperature coefficient of resistivity (K^{-1}) and ΔV is the CCA voltage change with respect to the reference voltage (V).

For the gap velocity measurements, the temperature derivative in Eq. (4) i.e. $\left.\frac{\partial E}{\partial T}\right|_U$ will firstly be determined. The gap velocity probe is positioned at a certain radial position in the calibration rig. The reference (ambient) temperature of the probe is taken by placing a portable K-type thermometer between the rotating and stationary plates. By keeping the motor speed, radial position of the probe and the gap between the disks constant, the output of the CTA and CCA are taken at the interval of 5 minutes. After at least seven sets of readings, the temperature derivative in Eq. (4) can be obtained. The calibration constants for the hot wire in Eq. (3) will then be determined by varying the speed of the motor but keeping *r* and *d* constant. A sample of 999 voltages each from the CTA and CCA are digitized by a 12-bit analog-to-digital converter before being input into a computer for processing. Both the temperature derivative and the calibration constants are obtained by least squares method, and fed into the second part of a computer program which converts the hot-wire voltage into velocity; the mean value is then determined from the 999 samples. To reduce the effect of wire drift, the duration between successive calibrations is kept within 1 hour.

After the gap velocity probe has been calibrated in the calibration rig, the probe is transferred and inserted into the front volute cover of the pump. Only one gap velocity probe was used at a time. This is to prevent the interruptions on the internal surface of the pump casing which could create eddies. Note that the other six holes are flushed with the Perspex cover during measurement. After ensuring that there was no obstruction in the pump, the motor was started with the speed set at 361rpm. Then, seventy-two velocity measurements were taken at an interval of 5°. The steps are repeated for the other 6 radial positions. The present experiment is done at operating condition, which has the inlet flow coefficient of $\Phi = Q/(2\pi r^2 b\omega) = 0.04$ (where Q is the inlet flowrate, b is the width of the impeller vane and r is the radius of the impeller) that is corresponding to the flowrate of 7 l/min of prototype pump.

Results and discussion

Figure 5 shows the tangential velocity distribution at ξ = 0.25. The distributions of tangential velocity have indicated clearly the effect of double-spiral volute of the pump on the flow in the gap. At the beginning, the fluid flow from the impeller is being blocked by the cutwater and there is only small amount of fluid flow from the volute to the gap.

Using Laser Doppler Anemometer, Leo [10] has measured the flow between the 16 forward blade impeller in a 5:1 model pump with water as medium. It was found that the flow at the beginning of the location of both cutwater (θ = 0°) and splitter plate (θ = 180°) were being blocked and bounced back due to the small space between the double volute and the impeller. Note that the definition of the reference angle at θ = 0° can be found at the upper right hand corner of Figure 8. In addition, most of the fluid has been discharged at the outlet of the pump which is at θ = 0°. These have explained why the tangential velocity is reducing from θ = 0° to θ = 120°. From θ = 120° onwards, there

are more fluid flow out from the impeller to the volute and available from

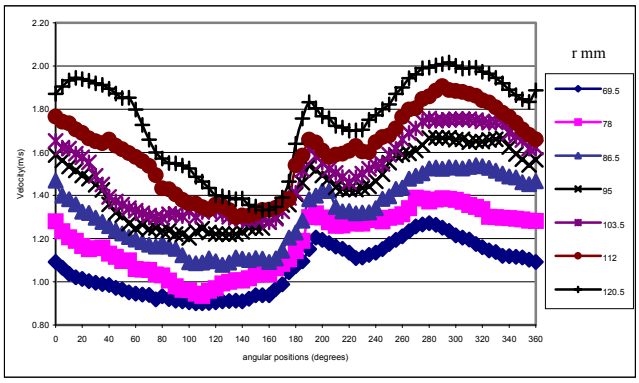

Figure 5. Tangential gap velocity in Cartesian plot for $\xi = 0.25$

the volute to the gap. This is due to the gradual space increment between the impeller and the volute. This is reflected in the distributions of the flow from $\theta = 120^o$ to $\theta = 150^o$ that the velocity has stopped decreasing and maintaining at about the same level or even start to increase. In addition, the increase of the velocity from $\theta = 150^o$ to $\theta = 190^o$ is due to the greatest opening space in between the impeller and the volute. As the starting location of the splitter plate is at $\theta = 180^o$, it is then not unexpected that flow is blocked and the velocity is decreasing again from $\theta = 190^o$ to $\theta = 220^o$. The about 10^o delay in the decreasing of the velocity is due to the present flow condition, with sufficient fluids at the gap. The increase of velocity from there onwards is due to that there are bigger space between the impeller and the splitter plate. On the whole the higher level of tangential velocity from $\theta = 180^o$ to $\theta = 360^o$ as compared to those from $\theta = 0^o$ (or $\theta = 360^o$) to $\theta = 180^o$ is due to that most of the fluids will be out of the pump from the volute at $\theta = 0^o$, i.e. the leakage flow to the gap is naturally reduced.

The distributions of radial velocity as shown in Figure 6 indicate that the velocity increase with the increase of radial location and basically there is no cross flow in between the distribution.

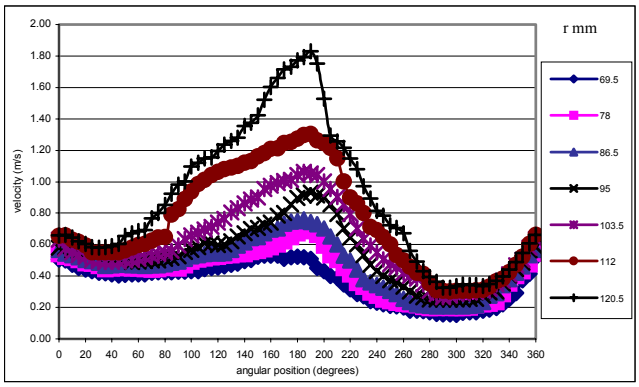

Figure 6. Radial gap velocity in Cartesian plot for $\xi = 0.25$

In general, the radial velocity is relatively smaller and the variation is not as drastic as the tangential velocity except at the two highest radial locations namely 112mm and 120.5mm. However, the radial velocity is the component, which lead the fluid flow in the direction towards the eye of the impeller. It is important that the fluid flow out from the gap, so that the blood will not keep on rotating in the gap and subjecting to higher risk of hemolysis. The relative high magnitude of radial velocity is distributed from $\theta = 80^o$ to $\theta = 240^o$. The high radial velocity at these locations has directed the fluid flow towards the eye. These have indicated the influence of splitter plate on the velocity distribution.

With the tangential and radial velocity, the resultant gap velocity V and its direction θ_r can then be computed by:

$$V = \sqrt{u^2 + v^2} \tag{6}$$

$$\theta_r = \tan^{-1}(v/u) \tag{7}$$

Figures 7, 8 and 9 show the vector plot of the resultant velocity at $\xi = 0.25$, 0.5 and 0.75 respectively. In the plot, the vector magnitude, V is represented by the vector length by a scale factor of Grid Units / Vector magnitude equal to 10. The head of the vector is positioned at the data point. It can be observed that the fluid flow in the clearance gap is generally in tangential direction with a very slight tilting towards the eye. The only exception is the velocity vectors distributed from $\theta = 100^o$ to $\theta = 190^o$. The high radial velocity in this region has strongly influenced the flow to direct to the eye of the impeller has formulated a washout mechanism that flush the blood to the eye of the impeller. The velocity vector distributions have demonstrated the good washout at the gap with no trace of flow reversal or vortex formed. These have explained why the Kyoto-NTN pump has less hemolysis as compared to other bio-pump.

The gap velocity increases towards the splitter plate and decreases after that. Indicating that the flow has been blocked at the splitter plate and is starting to reduce in the inner volute, and thus less fluid is available at the region after 180^o angular position. The location of the splitter plate at $\theta = 180^o$ although has reduced the fluid from the impeller to the splitter plate, its existence has however provided a mechanism to force the earlier fluid (those flow from $\theta = 100^o$ until about $\theta = 180^o$) to flow more towards the eye.

For the inner volute flow, the fluid flow is increasing with the slowly increased space between the splitter plate and the impeller. The fluid flow follows the inner volute to the cutwater, which is at the exit. In this region ($\theta = 320^o$ to $\theta = 40^o$), the fluid flow is directed to the discharge tube of the pump model and thus the gap flow is not as much as for the region from $\theta = 120^o$ to $\theta = 240^o$.

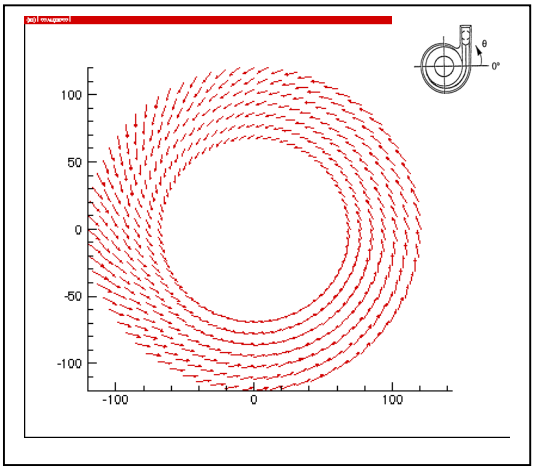

Figure 7. Gap velocity in vector plot for $\xi = 0.25$

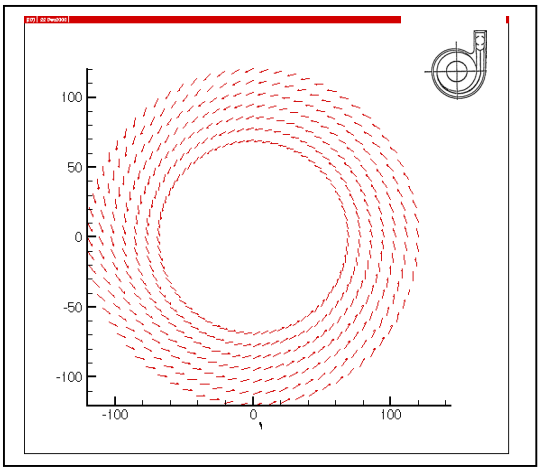

Figure 8. Gap velocity in vector plot for ξ = 0.50

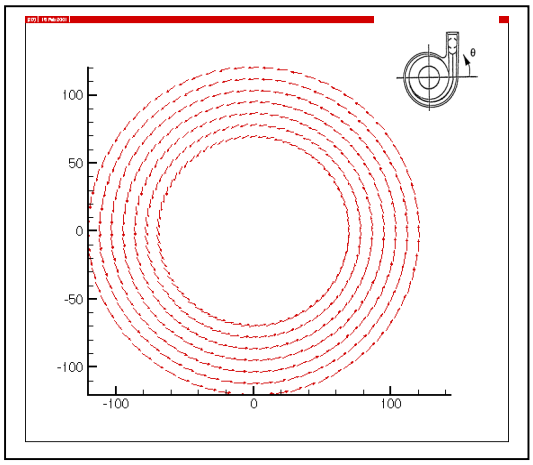

Figure 9 Gap velocity in vector plot for ξ = 0.75

However, it can be observed that the washout mechanism becomes weaker with the increase of ξ. From the vector it can be observed that at higher ξ especially for 0.75, the fluid flow is generally directed in tangential direction. This is due to the strong effect of the impeller which is having the turning motion in tangential direction.

Conclusion

Measurements of the tangential and radial velocity of the fluid flow in the 1.0 mm clearance gap between the impeller face and inlet casing of the blood pump model was completed at ξ = 0.25, 0.50 and 0.75 at operating condition. The velocity vector distributions indicated a good washout of blood flow and would prevent thrombosis in the clearance gap. It would flush the fluid towards the eye of the impeller. However, this mechanism becomes weaker with the increase of ξ. At high ξ, the tangential velocity is the dominant component due to the rotating motion of the impeller. The double-spiral volute design has significantly affected the fluid flow in the clearance gap. The location of the splitter plate and the cutwater is decisive on the washout mechanism of the pump. It can be observed that the velocity in the region before and after the splitter plate ($\theta = 180^{o}$) is distinctly flowing towards the eye of the impeller than in other angular locations. Hence, any further improvement on the performance of the blood pump should be focused on the adjustment of the locations and the profile of the double-spiral volute.

References

[1] Akamatsu, T., Tsukiya, T., Fluid dynamics design of Kyoto-NTN magnetically suspended centrifugal blood pump, ASME Fluids Engineering Division Summer Meeting, June, FEDSM97-3425, 1997, 22-26.

[2] Akamatsu, T., Centrifugal blood pump with a magnetically suspended impeller, Artif. Organs.,**16(3)**, 1992, 290-301.

[3] Akamatsu, T., Tsukiya, T., Nishimura, K., Park, C.H., Nakazeki, T., Recent studies of the centrifugal blood pump with a magnetically suspended impeller, Artif. Organs.,**19(7)**, 1995, 631-634.

[4] Chua, L.P., Akamatsu, T., Chan, W.K., Int. Comm. Heat Mass Transf., **16(3)**, 1998, 1055.

[5] Perry, A.E., How-wire anemometry. Oxford, University Press, New York, 1982.

[6] Chua, L.P. and Akamatsu, T., Measurements of Gap Pressure and Wall Shear Stress of a Blood Pump Model. Medical Engineering and Physics., **(22)**, 2000, 175-188.

[7] Chua, L.P., Tung, S.C., Chan, W.K., Int. Comm. Heat Mass Transf., **(26)**, 1999, 65.

[8] Brown, G.L., Davey, R.F., The calibration of hot films for skin friction measurement, Review of Scientific Instr., **42(11)**, 1971, 1729-31.

[9] Geremia, J.O., Disa Inform., 1972, 13, 5.

[10]Leo, H.L., Measurement of an enlarged blood pump model. Master of Engineering Thesis. School of Mechanical and Production Engineering, Nanayang Technological University, Singapore., 2000